Electron Spin Resonance, Magnetic, and X-ray Crystallographic Studies of a Binuclear, Imidazolate Bridged Copper(II) Complex, $[(TMDT)_2Cu_2(im)(ClO_4)_2](ClO_4)$[1]

Chi-Lin O'Young,[2a] John C. Dewan,[2a] Henry R. Lilienthal,[2b] and Stephen J. Lippard*[2a]

Contribution from the Department of Chemistry, Columbia University, New York, New York 10027, and the Physical Sciences Department, T. J. Watson Research Center, Yorktown Heights, New York 10598. *Received May 2, 1978*

Abstract: The syntheses of the mononuclear $[(TMDT)Cu(NO_3)](PF_6)$, $[(TMDT)Cu(1\text{-MeIm})](ClO_4)_2$, and binuclear $[(TMDT)_2Cu_2(im)(ClO_4)_2](ClO_4)$ complexes, where TMDT = 1,1,7,7-tetramethyldiethylenetriamine, 1-MeIm is 1-methylimidazole, and im is the imidazolate ion, are described. Single-crystal X-ray diffraction studies of the binuclear complex revealed the geometry of the imidazolate bridged dicopper(II) center. Each copper is pentacoordinate, with a bridging imidazolate and three TMDT nitrogen atoms forming an approximate plane and a perchlorate oxygen atom in the apical position of a distorted tetragonal pyramid. The bridging ligand is nearly perpendicular to both copper coordination planes and steric interactions restrict rotation about the Cu-N1 and Cu-N3 bonds, which have respective distances of 1.944 (12) and 1.966 (14) Å. The two copper mean coordination planes intersect at an angle of 148.7°. Two weakly coordinated, axial perchlorate ligands, the two N-H protons of the TMDT ligands, and the C2-H proton of the bridging imidazolate ligand all occupy space on one side (inside the shallow "V") of the binuclear complex. The Cu-Cu distance is 5.935 (4) Å. Variable temperature (4.2-295 K) magnetic susceptibility data for the bridged complex show an antiferromagnetic exchange interaction with a coupling constant ($\mathcal{H}' = -2J\mathbf{S}_1\cdot\mathbf{S}_2$) $J = -25.80$ (16) cm^{-1}. The exchange interaction is also apparent in the powder ESR spectrum which has a weak $\Delta M = 2$ transition exhibiting well-resolved copper hyperfine coupling and a characteristic line shape for the $\Delta M = 1$ transition. Temperature and pH dependent ESR and optical spectroscopic studies of frozen 50% aqueous Me_2SO solutions of all three complexes have also been carried out and show that the bridged cation $[(TMDT)_2Cu_2(im)(ClO_4)_2]^+$ exists as a major species in solution over the fairly narrow range $8.5 \lesssim pH \lesssim 9.5$. At low pH the bridge is broken and eventually free cupric ion forms; hydroxide ion is capable of breaking the bridge in alkaline solutions. The magnetic and ESR spectral properties of the binuclear complex are in excellent agreement with those of bovine erythrocyte superoxide dismutase in which copper(II) is substituted for zinc(II).

Discrete imidazolate (im) bridged metal complexes are of interest for several reasons. First, the synthesis and study of imidazolate bridged complexes will facilitate the identification and characterization of histidine bridged metal centers in metalloproteins. A histidine bridged copper(II)-zinc(II) active site (**1**) occurs in each of the two identical subunits of

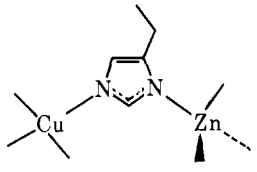

1

the enzyme bovine erythrocyte superoxide dismutase (BESOD).[3] A histidine bridge has also been postulated to link high-spin iron(III) heme and copper(II) centers in cytochrome *c* oxidase.[4] Second, splitting of the histidine bridge has been postulated to occur during BESOD turnover.[5] Studies of bimetallic imidazolate bridged complexes would therefore afford a means of testing this feature of the enzyme mechanism in a model system. Third, it is desirable to obtain magnetic data on discrete, imidazolate bridged complexes in the solid state since magnetic interaction through bridging nitrogen heterocyclic ligands is a topic of much current activity.[6] Finally, solution spectroscopic, magnetic, and chemical reactivity studies of soluble, binuclear imidazolate bridged species will enhance our general understanding of ligand bridged metal clusters.

Although binuclear metal complexes bridged by nitrogen-containing heterocycles such as pyrazine[7] were known, analogous imidazolate bridged species remained elusive,[8] despite the fact that oligomeric and polymeric imidazolate bridged metal complexes are quite common in the solid state.[9] Following reports[10,11] from this laboratory of water-soluble, imidazolate bridged dicopper(II) complexes, however, several such compounds have been obtained as crystalline solids and/or characterized as discrete species in solution. There now exist well-defined units **2** where M is copper,[10-12] heme iron,[13] mercury,[14] and ruthenium.[15]

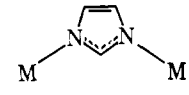

2

Our initial efforts concentrated on copper(II) complexes, specifically **3**, **4**, and **5**,[10,11] since magnetic exchange interactions facilitate identification of bridged compounds both in the solid state and in solution. Moreover, an active derivative of BESOD has been prepared in which Cu(II) is substituted for Zn(II).[16] The availability of ESR spectroscopic and magnetic data on this derivative permits evaluation of **3**-**5** as model compounds. Studies were also carried out using 1,1,7,7-tetramethyldiethylenetriamine as a ligand. In this paper we describe (1) the synthesis of the imidazolate bridged complex **6**; (2) its characterization in the solid state by X-ray crystallography, magnetic susceptibility studies, and ESR spectroscopic measurements; and (3) solution ESR experiments that define the pH range over which the imidazolate bridge is stable. Complex **6** is shown to have essentially the same temperature-dependent magnetic susceptibility and solution ESR spectral properties as the 4-Cu(II) form of BESOD.

Experimental Section

Materials and Methods. All compounds were prepared from commercially available starting materials used without further purification. Microanalyses were performed by Galbraith Laboratories, Knoxville, Tenn. Melting points were obtained by packing standard

0002-7863/78/1500-7291$01.00/0

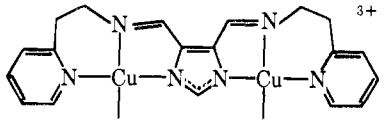

Cu_2bpim^{3+}

3

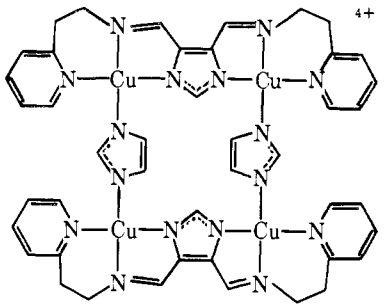

$[Cu_2(bpim)(im)]_2^{4+}$

4

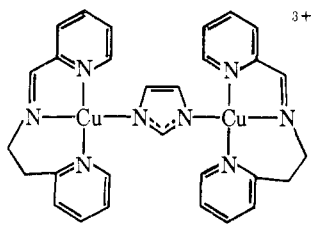

$[Cu(pip)]_2(im)^{3+}$

5

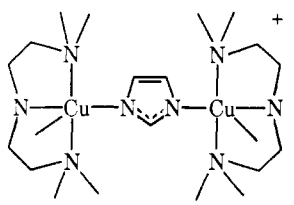

$[(TMDT)_2Cu_2(im)(ClO_4)_2]^+$

6

capillaries and are uncorrected. A Radiometer TTT 1C pH meter was used to determine the pH of aqueous solutions.

Variable-temperature (4.2 K < T < 295 K) magnetic susceptibility measurements were made by the Faraday method at seven different field strengths in the range 6–18 kOe. Magnetic susceptibilities at each temperature were determined from the slope of a plot of moment vs. field. The near-zero intercepts of these plots showed the absence of ferromagnetic impurities. A description of the apparatus and further experimental details may be found in ref 17. Diamagnetic corrections were applied using tabulated constants and the temperature-independent paramagnetism was taken to be 60×10^{-6} cm^3 g-atom-(Cu)$^{-1}$.[9p,18]

A Varian E-line X-band spectrometer operating in the 9.152–9.232-GHz range was used to record the electron spin resonance spectra. The g values were calibrated with diphenylpicrylhydrazil (DPPH, g = 2.0036) sealed in a quartz capillary as an external standard and placed in the ESR cavity alongside the sample. Samples were dissolved in water to known concentrations and the pH of a 1-2-mL aliquot was adjusted with a few drops of concentrated HNO_3 or NaOH. Unless otherwise noted, dimethyl sulfoxide (50% by volume) was added to assure the formation of rigid glasses at low temperatures. The final solution concentrations ranged from 5 to 10 mM and have not been corrected for dilution effects during the pH adjustment step. The temperature was controlled with an Air Products LTD-3-110 liquid helium cryostat. Temperatures were measured before and after each spectrum with a calibrated carbon resistor positioned in the sample compartment.

Solution electronic spectra were recorded with a Cary-118C spectrophotometer using 1-cm matched quartz cells. Except where noted otherwise, solution concentrations are approximate and were determined as described above for the ESR spectral studies. Infrared spectra of solids pressed into KBr pellets were measured using a Perkin-Elmer Model 283 instrument and were calibrated with polystyrene film.

Preparation of Compounds. μ-Imidazolato-bis(perchlorato-1,1,7,7-tetramethyldiethylenetriaminecopper(II)) Perchlorate, [(TMDT)$_2$Cu$_2$(im)(ClO$_4$)$_2$](ClO$_4$) (6). A. A solution of 318 mg (2 mmol) of TMDT in 2 mL of methanol was added to 10 mL of a methanol solution containing 483 mg (2 mmol) of $Cu(NO_3)_2 \cdot 3H_2O$. To the resulting mixture were added 68 mg (1 mmol) of imidazole dissolved in 2 mL of 0.5 N NaOH followed by 843 mg (6 mmol) of $NaClO_4 \cdot H_2O$ in 10 mL of methanol. After standing overnight, the solution deposited a blue precipitate which was collected by filtration, washed with methanol, and dried in vacuo over anhydrous calcium sulfate. The yield was 260 mg (32%). Single crystals suitable for X-ray diffraction study were obtained by slow evaporation of an aqueous solution, mp 219 °C dec.

Anal. Calcd for $C_{19}H_{45}N_8Cl_3O_{12}Cu_2$, C, 28.14; H, 5.59; N, 13.82; Cl, 13.11; Cu, 15.67; O, 23.67. Found: C, 28.31; H, 5.62; N, 14.04; Cl, 12.98; Cu, 15.74; O (by difference), 23.31.

IR: 3246 (m), 2924 (m, br), 1482 (s, br), 1436 (vw), 1418 (w), 1400 (vw), 1319 (w), 1298 (w), 1242 (m), 1222 (w), 1095 (vs, br), 990 (s), 944 (s), 867 (m), 860 (m), 783 (s), 698 (m), 676 (m), 623 (s), 487 (m), 420 (w), 364 (w), 320 (w) cm^{-1}.

B. Substitution of 741 mg (2 mmol) of $Cu(ClO_4)_2 \cdot 6H_2O$ dissolved in 10 mL of methanol for the cupric nitrate and sodium perchlorate solutions in A gave the same product in 39% yield (316 mg).

Anal. Found: C, 28.09; H, 5.42; N, 13.66; Cl, 12.95.

1-Methylimidazole-1,1,7,7-tetramethyldiethylenetriaminecopper(II) Perchlorate, [(TMDT)Cu(1-MeIm)](ClO$_4$)$_2$. A solution of 318 mg (2 mmol) of TMDT in 2 mL of methanol was added to 10 mL of 741 mg (2 mmol) of $Cu(ClO_4)_2 \cdot 6H_2O$ dissolved in 10 mL of methanol. Addition of a solution of 1-MeIm (246 mg, 3 mmol, in 2 mL of methanol) to the mixture produced a blue precipitate that was filtered, washed with methanol, and dried in vacuo over anhydrous calcium sulfate. The yield was 544 mg (54%). The compound was recrystallized from hot methanol, mp 187 °C (dec 198 °C).

Anal. Calcd for $C_{12}H_{27}N_5Cl_2O_8Cu$: C, 28.61; H, 5.40; N, 13.90; Cl, 14.07. Found: C, 28.67; H, 5.47; N, 13.68; Cl, 14.25.

IR: 3244 (m), 3140 (m), 2924 (s, br), 1550 (m), 1478 (s, br), 1454 (vw), 1431 (w), 1400 (vw), 1296 (m), 1246 (m), 1218 (vw), 1101 (vs, br), 988 (m), 941 (m), 932 (m), 863 (m), 846 (w), 778 (m), 664 (m), 623 (s), 490 (m) cm^{-1}.

Nitrato-1,1,7,7-tetramethyldiethylenetriaminecopper(II) Hexafluorophosphate, [(TMDT)Cu(NO$_3$)](PF$_6$). To a mixture of 483 mg (2 mmol) of $Cu(NO_3)_2 \cdot 3H_2O$ and 318 mg (2 mmol) of TMDT in 15 mL of methanol was added a solution of 334 mg (2 mmol) of sodium hexafluorophosphate in 5 mL of water. The resulting blue precipitate was washed with methanol and dried in vacuo over anhydrous calcium sulfate. The yield was 361 mg (42%). The compound was recrystallized from acetonitrile, mp 204 °C dec.

Anal. Calcd for $C_8H_{21}N_4PF_6O_3Cu$: C, 22.36; H, 4.93; N, 13.04. Found: C, 22.55; H, 5.30; N, 13.06.

IR: 3222 (s), 2936 (s, br), 1483 (vs, br), 1455 (w), 1440 (w), 1420 (w), 1388 (w), 1283 (s), 1220 (w), 1190 (vw), 1140 (w), 1104 (w), 1060 (w), 1040 (vw), 1028 (w), 990 (m), 942 (m), 842 (vs, br), 807 (m), 780 (m), 740 (w), 715 (vw), 556 (s), 506 (w), 426 (w), 363 (vw), 295 (w), 272 (vw) cm^{-1}.

Collection and Reduction of X-ray Data. The dark blue crystal used for the diffraction study was a hexagonal plate bounded by (001) and (00$\bar{1}$), 0.034 mm apart; (100) and ($\bar{1}$00), 0.168 mm apart; and the {110} faces, 0.206 mm apart. Preliminary precession and Weissenberg photographs (Cu Kα radiation, λ 1.5418 Å) showed the lattice to have Laue symmetry $2/m$ with extinctions $0k0$ when $k \neq 2n$, consistent with space groups $C_2^2 - P2_1$ and $C_{2h}^2 - P2_1/m$.[19] The quality of the data crystal was examined by taking open counter ω scans of several strong, low-angle reflections. Although these peaks showed some structure, there was much less than for previous batches of crystals examined over a period of several months. Since this batch was superior, it was decided to proceed. The details of data collection and reduction are given in Table I.

Determination and Refinement of the Structure. The structure was solved by conventional heavy atom methods from Patterson and Fourier maps. The solution to the Patterson map, computed using all data, was consistent only with the noncentrosymmetric space group $P2_1$. Neutral atom scattering factors for the nonhydrogen atoms and

Table I. Experimental Details of the X-ray Diffraction Study of $[(TMDT)_2Cu_2(im)(ClO_4)_2](ClO_4)$

A. Crystal Parameters[a] at 23 °C

a = 17.087 (12) Å	mol wt 811.1
b = 11.757 (7) Å	space group $P2_1$
c = 8.423 (6) Å	Z = 2
β = 97.06 (4) °	ρ (calcd) = 1.604 g/cm^3
V = 1679.3 Å^3	ρ (obsd)[b] = 1.598 (7) g/cm^3

B. Measurement of Intensity Data

instrument: Picker FACS-1-DOS diffractometer
radiation: Mo Kα (λ_{α_1} 0.7093 Å), graphite monochromatized
takeoff angle: 2.0°
detector aperture: 6.3 × 6.3 mm
crystal-detector distance: 33 cm
scan technique: coupled θ (crystal)-2θ(counter)
scan range: 2.0° (symmetric, plus Kα1-Kα2 dispersion)
scan rate: 1°/min
maximum 2θ: 45°, above which there were few observable reflections
background measurements: stationary crystal stationary counter; 20-s counts at each end of 2θ scan range
standards: three reflections (020), ($\bar{2}$01), and (2$\bar{1}$0) measured after every 97 data reflections showed only random, statistical fluctuations
no. of reflections collected: [2$\theta \leq 20°$ ($\pm h$, $+k$, $\pm l$), $20 < 2\theta < 45°$ ($+h$, $+k$, $\pm l$)]; 2362 unique, non-space group extinguished

C. Treatment of Intensity Data[c]

reduction to preliminary F_o^2 and $\sigma(F_o^2)$: correction for background, attenuators, and Lorentz-polarization of monochromatized X-radiation in the usual manner;[d] ϵ[e] = 0.04
absorption correction: μ = 15.7 cm^{-1}; transmission factors varied from 0.80 to 0.95
averaging: 301 equivalent pairs in the inner sphere ($2\theta \leq 20°$); agreement factor R_{av}[f] = 0.021
scaling: Wilson's method[g]
observed data: 1710 unique reflections for which $F_o^2 > 2\sigma(F_o^2)$

[a] From a least-squares fit to the setting angles of 12 reflections. [b] By suspension in a mixture of bromoform and chloroform. [c] Programs for an IBM 360/91 computer used in this work: AVERAGE, which computes a weighted average of equivalent reflections and was written by J. T. Gill; XDATA, the Brookhaven-Wilson plot and scaling program; ORABS, the local version of the Oak Ridge absorption correction program; FOURIER, a modification of the Zalkin FORDAP program by R. J. Dellaca and W. T. Robinson, further modified by D. J. Hodgson; CUGLS, the Columbia University version of the Busing-Martin-Levy structure factor calculation and least-squares refinement program, ORFLS; ORFFE, the Busing-Martin-Levy molecular geometry and error function program; ORTEP II, the Johnson thermal ellipsoid plotting program; and various local data processing programs. [d] J. T. Gill and S. J. Lippard, *Inorg. Chem.*, **14**, 751 (1975). [e] P. W. R. Corfield, R. J. Doedens, and J. A. Ibers, *ibid.*, **6**, 197 (1967). [f] $R_{av} = (\Sigma_{i=1}^{N} \Sigma_{j=1}^{n} |\bar{F}_i^2 - F_{ij}^2|)/\Sigma_{i=1}^{N} \bar{F}_i^2$, where N is the number of reflections measured more than once and n is the number of observations of the Nth reflection. [g] A. J. C. Wilson, *Nature (London)*, **150**, 151 (1942).

corrections for the anomalous dispersion effects for the copper and chlorine atoms were obtained from ref 20. Scattering factors for the hydrogen atoms were those of Stewart et al.[21]

Toward the final stages of least-squares refinement, with anisotropic thermal parameters assigned to copper and chlorine, the discrepancy factors had values of R_1 = 0.074 and R_2 = 0.081.[22] Most of the perchlorate oxygen atoms had large (7-17 Å^2) isotropic temperature factors and it was decided to refine these anisotropically even though doing so would reduce the data to variable parameter ratio from 8.5 to 6.5. Because of the paucity of data, the C and N atoms of the ligand were not refined anisotropically. After several cycles of such refinement, R_1 and R_2 were 0.066 and 0.065, respectively. Since $P2_1$ is a polar space group, refinement of the alternative absolute configuration was carried out. Based on the slightly superior[23] R factors of 0.065 and 0.064, respectively, and the better agreement of chemically equivalent copper-nitrogen distances for the two crystallographically independent coordination geometries, the second configuration was adopted. The hydrogen atoms on the central nitrogen atom of the TMDT ligands were located from a difference Fourier map and the remaining, nonmethyl hydrogen atoms were placed in calculated positions (C-H, 0.95 Å). These atoms were included as invariants with isotropic thermal parameters fixed at 5 Å^2. No attempt was made to locate the methyl group hydrogen atoms. In the final cycle of refinement, no parameter varied by more than 0.04 of its estimated standard deviation. The discrepancy indices R_1 and R_2 converged at 0.061 and 0.060, respectively.

The $|F_o| - |F_c|$ values for strong, low-order reflections were randomly positive and negative and therefore no corrections for secondary extinction were applied. In a test of the weighting scheme used, the function $w\Delta^2$ for data sectioned both with respect to $|F_o|$ and to (sin θ/λ) showed reasonable consistency and the weighting scheme was therefore considered to be satisfactory. The standard deviation of an observation of unit weight was 1.48.[23] A final difference Fourier map showed a peak of 0.75 e/Å^3 at a distance of 0.94 Å from methyl carbon atom C21. The remaining electron density was all less than 0.56 e/Å^3, the typical value for a hydrogen atom.

The final nonhydrogen atomic positional parameters are listed in Table II. The hydrogen atom positional parameters, the refined thermal parameters, the final observed and calculated structure factor amplitudes, and the root-mean-square thermal amplitudes for an-

Table II. Final Positional Parameters of the Atoms of $[(TMDT)_2Cu_2(im)(ClO_4)_2](ClO_4)$[a]

Atom	x	y	z
Cu1	0.84142 (11)	0	0.1063 (2)
Cu2	0.67471 (11)	−0.3916 (2)	−0.2271 (2)
C11	0.9441 (3)	−0.1902 (5)	0.3771 (7)
C12	0.7807 (4)	−0.5670 (6)	0.0592 (7)
C13	0.4447 (3)	0.6277 (5)	0.3442 (6)
O11	0.8939 (9)	−0.1712 (13)	0.2365 (16)
O12	0.9613 (8)	−0.3024 (15)	0.4070 (18)
O13	0.9055 (14)	−0.1510 (18)	0.503 (2)
O14	1.0061 (12)	−0.1249 (20)	0.371 (3)
O21	0.7665 (9)	−0.4595 (12)	−0.0130 (17)
O22	0.7112 (12)	−0.5997 (18)	0.115 (3)
O23	0.8326 (12)	−0.5663 (19)	0.194 (2)
O24	0.797 (2)	−0.6419 (18)	−0.045 (2)
O31	0.3937 (7)	0.6109 (18)	0.4580 (17)
O32	0.5092 (7)	0.6942 (12)	0.4171 (15)
O33	0.4066 (9)	0.6868 (12)	0.2081 (16)
O34	0.4704 (9)	0.5245 (13)	0.291 (2)
N1	0.7775 (7)	−0.0910 (11)	−0.0531 (15)
N11	0.9288 (8)	0.0349 (12)	−0.0384 (16)
N12	0.9064 (7)	0.0951 (13)	0.2667 (15)
N13	0.7540 (7)	0.0336 (12)	0.2437 (15)
N3	0.7201 (7)	−0.2392 (11)	−0.1854 (15)
N21	0.7427 (7)	−0.4332 (11)	−0.4069 (15)
N22	0.6213 (8)	−0.5386 (13)	−0.2836 (17)
N23	0.5790 (8)	−0.3633 (13)	−0.0967 (16)
C2	0.7693 (9)	−0.2039 (16)	−0.062 (2)
C4	0.6921 (10)	−0.1445 (16)	−0.259 (2)
C5	0.7258 (10)	−0.0506 (15)	−0.178 (2)
C11	0.9602 (12)	−0.0737 (20)	−0.119 (2)
C12	0.8934 (10)	0.1214 (19)	−0.1641 (20)
C13	0.9956 (10)	0.0859 (16)	0.0677 (19)
C14	0.9627 (10)	0.1642 (15)	0.187 (2)
C15	0.8547 (9)	0.1608 (15)	0.361 (2)
C16	0.7894 (10)	0.0844 (16)	0.395 (2)
C17	0.6962 (10)	0.1195 (19)	0.1562 (20)
C18	0.7058 (11)	−0.0689 (18)	0.280 (2)
C21	0.8304 (11)	−0.4289 (18)	−0.357 (2)
C22	0.7209 (10)	−0.3578 (16)	−0.545 (2)
C23	0.7197 (11)	−0.5520 (17)	−0.457 (2)
C24	0.6369 (12)	−0.5750 (19)	−0.440 (3)
C25	0.5401 (10)	−0.5336 (16)	−0.249 (2)
C26	0.5388 (10)	−0.4732 (17)	−0.100 (2)
C27	0.5264 (12)	−0.275 (2)	−0.172 (3)
C28	0.6090 (11)	−0.3275 (17)	0.069 (2)

[a] Atoms are labeled as indicated in Figure 1. Standard deviations, in parentheses, occur in the last significant figure for each parameter.

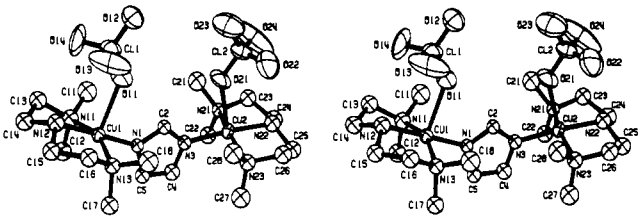

Figure 1. Stereoscopic view of the $[(TMDT)_2Cu_2(im)(ClO_4)_2]^+$ cation showing the 40% probability thermal ellipsoids and the atom labeling scheme.

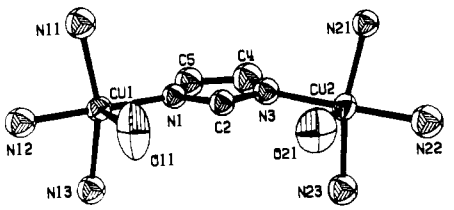

Figure 2. Imidazolate bridge and copper coordination geometry of the $[(TMDT)_2Cu_2(im)(ClO_4)_2]^+$ cation. The 50% probability thermal ellipsoids are displayed. Note that the carbon and nitrogen atoms were refined isotropically.

Table III. Interatomic Distances (Å) in $[(TMDT)_2Cu_2(im)(ClO_4)_2](ClO_4)$[a]

Coordination Sphere			
Cu1		Cu2	
Cu1-N1	1.944 (12)	Cu2-N3	1.966 (14)
Cu1-N11	2.081 (14)	Cu2-N21	2.078 (13)
Cu1-N12	1.985 (14)	Cu2-N22	1.986 (15)
Cu1-N13	2.038 (13)	Cu2-N23	2.105 (13)
Cu1-O11	2.412 (14)	Cu2-O21	2.379 (13)
Internal Ligand Geometry			
Cu1		Cu2	
N11-C11	1.57 (2)	N21-C21	1.51 (2)
N11-C12	1.54 (2)	N21-C22	1.48 (2)
N11-C13	1.49 (2)	N21-C23	1.50 (2)
C13-C14	1.52 (2)	C23-C24	1.47 (2)
C14-N12	1.48 (2)	C24-N22	1.44 (2)
N12-C15	1.48 (2)	N22-C25	1.45 (2)
C15-C16	1.49 (2)	C25-C26	1.45 (2)
N13-C16	1.47 (2)	N23-C26	1.46 (2)
N13-C17	1.54 (2)	N23-C27	1.47 (2)
N13-C18	1.51 (2)	N23-C28	1.49 (2)
Imidazolate Ring Geometry			
N1-C2	1.34 (2)	C4-C5	1.39 (2)
C2-N3	1.32 (2)	C5-N1	1.37 (2)
N3-C4	1.33 (2)		
Anion Geometry			
Cl1-O11	1.39 (1)	Cl2-O21	1.41 (1)
Cl1-O12	1.37 (2)	Cl2-O22	1.39 (2)
Cl1-O13	1.39 (2)	Cl2-O23	1.35 (2)
Cl1-O14	1.31 (2)	Cl2-O24	1.29 (2)
Cl3-O31	1.39 (1)	Cl3-O33	1.43 (1)
Cl3-O32	1.43 (1)	Cl3-O34'	1.38 (2)
Nonbonded Distances			
	Cu1-Cu2 5.935 (4)		
C11-C18	5.81 (3)	C21-C28	5.65 (3)
C12-C17	4.57 (2)	C22-C27	4.94 (3)

[a] Atoms are labeled as shown in Figure 1. Standard deviations, in parentheses, occur in the last significant figure for each parameter. Distances are not corrected for thermal motion.

Table IV. Bond Angles (deg) for $[(TMDT)_2Cu_2(im)(ClO_4)_2](ClO_4)$[a]

Coordination Sphere			
Cu1		Cu2	
N1-Cu1-N11	95.0 (6)	N3-Cu2-N21	95.8 (5)
N1-Cu1-N12	179 (1)	N3-Cu2-N22	174.7 (5)
N1-Cu1-N13	96.3 (5)	N3-Cu2-N23	94.5 (6)
N11-Cu1-N12	84.6 (6)	N21-Cu2-N22	84.4 (5)
N11-Cu1-N13	157.4 (6)	N21-Cu2-N23	163.2 (5)
N12-Cu1-N13	83.8 (5)	N22-Cu2-N23	84.2 (6)
O11-Cu1-N1	90.1 (5)	O21-Cu2-N3	87.8 (5)
O11-Cu1-N11	100.2 (6)	O21-Cu2-N21	95.6 (5)
O11-Cu1-N12	90.8 (5)	O21-Cu2-N22	97.5 (5)
O11-Cu1-N13	99.3 (6)	O21-Cu2-N23	98.0 (5)
Internal Ligand Geometry			
Cu1		Cu2	
Cu1-N11-C11	114 (1)	Cu2-N21-C21	115 (1)
Cu1-N11-C12	106.5 (9)	Cu2-N21-C22	109 (1)
Cu1-N11-C13	106 (1)	Cu2-N21-C23	106 (1)
C11-N11-C12	112 (1)	C21-N21-C22	110 (1)
C11-N11-C13	108 (1)	C21-N21-C23	109 (1)
C12-N11-C13	111 (1)	C22-N21-C23	108 (1)
N11-C13-C14	109 (1)	N21-C23-C24	112 (2)
C13-C14-N12	106 (1)	C23-C24-N22	109 (2)
C14-N12-C15	115 (1)	C24-N22-C25	119 (1)
Cu1-N12-C14	110 (1)	Cu2-N22-C24	110 (1)
Cu1-N12-C15	109.8 (9)	Cu2-N22-C25	110 (1)
N12-C15-C16	108 (1)	N22-C25-C26	108 (1)
C15-C16-N13	108 (1)	C25-C26-N23	113 (2)
Cu1-N13-C16	109 (1)	Cu2-N23-C26	104 (1)
Cu1-N13-C17	109.1 (9)	Cu2-N23-C27	111 (1)
Cu1-N13-C18	115 (1)	Cu2-N23-C28	110 (1)
C16-N13-C17	109 (1)	C26-N23-C27	111 (1)
C16-N13-C18	109 (1)	C26-N23-C28	112 (1)
C17-N13-C18	107 (1)	C27-N23-C28	109 (2)
Imidazolate Ring Geometry			
Cu1-N1-C2	129 (1)	Cu2-N3-C2	129 (1)
Cu1-N1-C5	126 (1)	Cu2-N3-C4	124 (1)
C2-N1-C5	104 (1)	C2-N3-C4	105 (1)
N1-C5-C4	107 (1)	N3-C4-C5	109 (1)
	N1-C2-N3 114 (2)		
Anion Geometry			
Cu1-O11-C11	132.6 (9)	Cu2-O21-C12	133.6 (9)
O11-C11-O12	114 (1)	O21-C12-O22	107 (1)
O11-C11-O13	107 (1)	O21-C12-O23	115 (1)
O11-C11-O14	107 (1)	O21-C12-O24	111 (1)
O12-C11-O13	107 (1)	O22-C12-O23	102 (1)
O12-C11-O14	114 (1)	O22-C12-O24	108 (2)
O13-C11-O14	107 (2)	O23-C12-O24	113 (2)
O31-C13-O32	107.3 (9)	O32-C13-O33	109.4 (9)
O31-C13-O33	111 (1)	O32-C13-O34	111.2 (9)
O31-C13-O34	110 (1)	O33-C13-O34	107 (1)

[a] See footnote *a*, Table III.

isotropically refined atoms are available as Tables S1-S4, respectively.[24] The structure of the $[(TMDT)_2Cu_2(im)(ClO_4)_2]^+$ cation is shown in Figure 1 along with the atom labeling scheme. The geometry of the core atoms and the imidazolate bridge in this cation appears in Figure 2. Figure S1[24] displays the unit cell packing in a stereoview. Tables III and IV report interatomic distances and angles, respectively. Least-squares best planes through the bridging imidazolate ring and the copper coordination planes are available as Table S5.[24]

Results

Description of the $[(TMDT)_2Cu_2(im)(ClO_4)_2](ClO_4)$ Structure. The crystal lattice consists of discrete $[(TMDT)_2Cu_2(im)(ClO_4)_2]^+$ cations and perchlorate anions. There are no unusually short interionic contacts and the lattice is primarily stabilized by ionic and van der Waals interactions. The closest

Table V. Temperature Dependence of the Magnetic Susceptibility per Cu Atom (cm^3 g-$atom^{-1}$) and of μ_{eff} (μ_B) = $2.8273(\chi'_A(cor)\cdot T)^{1/2}$ for Solid $[(TMDT)_2Cu_2(im)(ClO_4)_2](ClO_4)$

T, K	$10^5\chi'_A$[a]	$10^5\chi'_A$ (cor)[b]	μ_{eff}
4.20	36.7	12.7	0.07
7.87	25.3	12.5	0.09
9.55	23.3	12.8	0.10
11.77	37.7	29.2	0.17
14.34	79.8	72.8	0.29
18.05	138.1	132.5	0.44
22.16	244.2	239.6	0.65
27.35	343.5	339.8	0.86
31.32	393.2	390.0	0.99
35.52	422.5	419.7	1.09
38.90	445.3	442.8	1.17
44.13	456.6	454.3	1.27
49.81	428.4	426.4	1.30
54.37	444.5	442.6	1.39
58.69	432.7	431.0	1.42
62.55	424.6	423.0	1.45
66.48	414.3	412.8	1.48
77.61	386.4	385.1	1.55
133.47	268.9	268.2	1.69
156.33	229.9	229.3	1.69
190.17	192.2	191.7	1.71
207.96	179.8	179.4	1.73
231.43	165.4	164.9	1.75
272.97	142.1	141.7	1.76
294.74	134.2	133.9	1.78
294.83	135.3	134.9	1.78

[a] Field-independent susceptibility corrected for diamagnetism. [b] Corrected for paramagnetic impurity as described in the text.

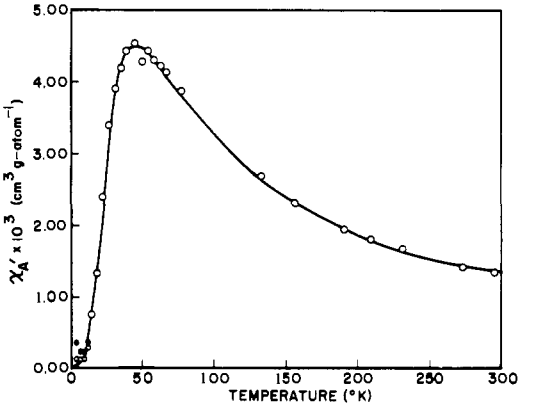

Figure 3. Susceptibility vs. temperature plot for solid $[(TMDT)_2Cu_2(im)(ClO_4)_2](ClO_4)$. Experimental data corrected for the presence of paramagnetic impurity are shown as open circles; filled circles indicate the uncorrected values where the correction is significant. The solid line shows the best least-squares fit to the data using the parameters described in the text.

approach between two copper atoms in different imidazolate bridged cations is 8.05 Å, which may be compared with the intracation distance of 5.935 (4) Å.

The packing of atoms within the binuclear cation (approximate point group symmetry C_{2v}) is quite compact, as may be seen from Figure 1 and by examination of a space-filling model. The eight methyl groups of the two TMDT ligands form a tight pocket about the copper atoms and prohibit rotation of the bridging imidazolate ion about the Cu-N1 and Cu-N3 bonds. The C5-C12, C5-C17, C4-C22, and C4-C27 distances range from 3.38 (3) to 3.56 (2) Å. The two perchlorate ions are attached on the same side of the copper coordination planes. These planes are canted at an angle of 148.7° with respect to each other. As a consequence, the two perchlorate ligands are rotated to avoid nonbonded repulsive interactions across the top of the bridging imidazolate ion (Figure 1). The two TMDT N-H protons and the C2-H proton of the imidazolate ligand are also situated on the perchlorate ion binding side of the cation. There are no strong intracation hydrogen bonding interactions, however. The fact that all the hydrophilic, polar groups occupy the same region of space within the cation may explain why another isomer, generated by a 180° rotation about the Cu2-N3 bond axis, does not exist in the crystal lattice. The presence of rotational isomers in solution could account for the difficulty in getting ordered crystals of imidazolate bridged dicopper(II) complexes.[25]

The coordination geometry including the bridging imidazolate ligand is depicted in Figure 2. Each copper atom is pentacoordinate, surrounded by an approximate plane of four nitrogen atoms from the TMDT and imidazolate ligands and by the oxygen atom of a perchlorate ion situated on the axis of a distorted tetragonal pyramid. While the constituent atoms of the imidazolate anion all lie within ±0.01 Å of the best mean plane through the ring, Cu1 and Cu2 are 0.02 and 0.35 Å, respectively, out of the plane. Such deviations are quite common in copper(II)-imidazole complexes.[26] Best plane calculations through the four nitrogen donor atoms at each copper center reveal departures from planarity of the kind generally observed for diethylenetriaminecopper(II) complexes.[27] In particular, N11 and N13 are both ~0.16 Å below the best mean plane through N11, N12, N13, and N1 while N12, N1, and Cu1 are 0.18, 0.15, and 0.18 Å, respectively, above that plane. Similar, but smaller, deviations from planarity [N21 (−0.07 Å), N23 (−0.07 Å), N22 (0.08 Å), N3 (0.06 Å), Cu2 (0.16 Å)] occur for the other copper coordination sphere. These values reflect a tetrahedral distortion of the four nitrogen atoms and movement of the copper atom out of the basal plane of the tetragonal pyramid toward the oxygen atom of the apical perchlorate ligand. The latter movement is not as great as often found in tetragonal pyramidal structures,[27e] however, owing to the fairly weak[28] Cu-O bonds (bond lengths = 2.412 (14) and 2.379 (13) Å). Bonding between the TMDT ligands and the copper atoms is normal, judging from the geometric parameters of Tables III and IV. The short copper to central nitrogen atom distances are typical.[27e] The average bond distance to the nitrogen atom of the bridging imidazolate ion, 1.955 (13) Å, may be compared with similar bonds having values of 1.964 (10) Å in **4**,[10] 1.976 (7) Å in $Cu_3(imH)_8(im)_2(ClO_4)_4$,[9m] and 1.975 (11) Å in $Cu(imH)_2(im)Cl$.[9n] The angles (α_1 and α_2)[11] between the plane of the bridging imidazolate ring and the coordination planes are 91.8 and 90.0° for Cu1 and Cu2, respectively.

The internal geometry (Tables III and IV) of the TMDT ligand and the bridging imidazolate ion is normal and agrees with numerous studies performed previously.[9,10,26,27] The precision of the present determination is not high, owing to the poor quality of even the best crystal available. The N-CH_3 bonds are slightly larger than expected since hydrogen atoms were not included for the terminal methyl groups. The perchlorate ion dimensions are also within a few standard deviations of the expected values.[28] No significance is attached to the short Cl1-O14 and Cl2-O24 distances (Table III) which have not been corrected for thermal motion (Figure 1).

Magnetic Susceptibility of Solid $[(TMDT)_2Cu_2(im)(ClO_4)_2](ClO_4)$. The field independent magnetic susceptibility per gram atom of copper, χ_A', at various temperatures is given in Table V for the solid perchlorate salt of **6**. A plot of χ_A' vs. T may be seen in Figure 3. The susceptibility of $[(TMDT)_2Cu_2(im)(ClO_4)_2](ClO_4)$ passes through a maximum ~48 K and then falls to a minimum ~9 K. This behavior is typical of an antiferromagnetically coupled compound with a small amount of paramagnetic impurity.[29] The slope of a plot of χ_A' vs. $1/T$ at temperatures below the minimum gave the Curie susceptibility of the impurity, $\chi_{impurity} = 1.008 \times 10^{-3}/T$ cm^3

Table VI. ESR Spectral Parameters and Selected Optical Spectral Data[a]

[(TMDT)Cu(NO$_3$)](PF$_6$)			[(TMDT)Cu(1-MeIm)](ClO$_4$)$_2$			[(TMDT)$_2$Cu$_2$(im)(ClO$_4$)$_2$](ClO$_4$)			
pH	$g_\parallel$	$A_\parallel$, G ($\times 10^4$ cm^{-1})	pH	$g_\parallel$	$A_\parallel$, G ($\times 10^4$ cm^{-1})	pH	$g_\parallel$	$A_\parallel$, G ($\times 10^4$ cm^{-1})	λ_{max}, nm
2.1	2.410	119 (134)	2.3	2.409[b]	119 (134)	2.3	2.412[b]	119 (134)	648
3.1	2.403[b]	118 (132)		2.230	180 (187)		2.232	180 (188)	
	2.240	180 (188)	2.6	2.409	120 (135)	3.7	2.412	120 (135)	642
4.0	2.406	118 (133)		2.230	180 (187)		2.232[b]	180 (188)	
	2.233[b]	179 (187)	3.2	2.409	120 (135)	5.3	2.232	180 (188)	633
4.8	2.235	180 (188)		2.230[b]	181 (188)	8.1	2.218	180 (186)	615
6.2	2.230	180 (187)	7.5	2.233	180 (188)	9.0	[c]	[c]	612
7.3	2.235	180 (188)	8.8	2.212	180 (186)	10.0	2.225	169 (176)	614
8.2	2.233	180 (188)	9.8	2.228	175 (182)	10.5	2.226	169 (176)	615
9.1	2.227	171 (178)	11.2	2.229	170 (177)	11.4	2.226	170 (177)	627
11.2	2.230	170 (177)							

[a] In 50% aqueous dimethyl sulfoxide solutions frozen at 77 K for ESR or at ambient temperature for optical spectral measurements. The solution concentrations were all ~5 mM. $A_\parallel$ values are reported both in gauss and in cm^{-1} ($\times 10^4$). [b] Major spectral component. [c] Mostly **6**; too little mononuclear species to observe.

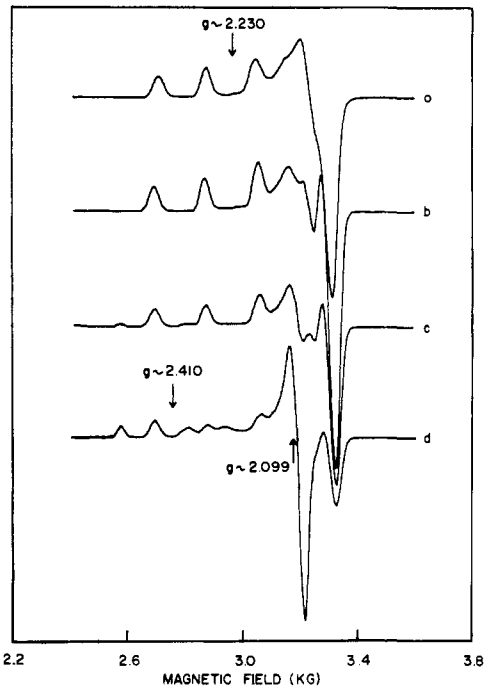

Figure 4. The ESR spectra of ~5 mM frozen (77 K) 50% aqueous Me_2SO solutions of [(TMDT)Cu(NO$_3$)](PF$_6$) at (a) pH 11.2, (b) pH 7.3, (c) pH 4.0, and (d) pH 3.1. Instrumental settings were 15 mW of microwave power, 5 G modulation amplitude, time constant of 0.3 s, and a sweep rate of 1000 G/min.

g-atom^{-1}. The impurity susceptibility would be accounted for by $\lesssim$0.25% of Cu(II) with μ_{eff} = 1.8 μ_B. The corrected susceptibilities, $\chi_A'(cor) = \chi_A' - \chi_{impurity}$, are given in Table V and Figure 3.

The corrected susceptibilities were fit to the expression[29,30]

$$\chi_A'(cor) = (g^2N\beta^2/kT)[3 + \exp(-2J/kT)]^{-1} + 6.0 \times 10^{-5} \quad (1)$$

by a nonlinear least-squares method in which g^2 and J were refined as variable parameters. Here J is the scalar coupling constant in the Heisenberg-Dirac-van Vleck Hamiltonian $\mathcal{H}' = -2J\mathbf{S}_1\cdot\mathbf{S}_2$, g is the average g value of the electron, and the other symbols have their usual meaning. The refinement converged at values of g = 2.085 ± 0.006 and J = −25.80 ± 0.16 cm^{-1} with a correlation coefficient of 0.9993. The calculated susceptibility vs. temperature curve is shown in Figure 3.

Electron Spin Resonance Spectra. [(TMDT)Cu(NO$_3$)](PF$_6$). The 77 K ESR spectra of this complex in frozen 50% aqueous Me_2SO solutions as a function of pH are displayed in Figure 4. Spectral parameters are summarized in Table VI. The ESR spectra reflect the presence of at least three different axially or nearly axially symmetric species in solution, possibilities for which are **7**–**9**.[31] At low pH, it is likely that the TMDT ligand

[(TMDT)Cu(H$_2$O)]$^{2+}$ **7** [(TMDT)Cu(OH)]$^+$ **8** [Cu(H$_2$O)$_6$]$^{2+}$ **9**

is dissociated according to[31]

$$\mathbf{7} \underset{\text{pH } \sim 2.6}{\overset{3H^+}{\rightleftharpoons}} \mathbf{9} + H_3(TMDT)^{3+} \quad (2)$$

The presence of **9** was verified by observing $g_\parallel$ and $g_\perp$ signals at 2.412 and 2.099, respectively, with $A_\parallel$ = 119 G, for a frozen solution of cupric perchlorate dissolved in the same solvent. At intermediate pH values the $g_\parallel$ and $A_\parallel$ parameters reveal the presence of both **9** and **7**, the latter having $A_\parallel$ ~180 G. As the pH increases above 9, the $A_\parallel$ value diminishes to 170 G, suggesting displacement of water by hydroxide ion, and at higher pH values a brown precipitate forms, eq 3.

$$\mathbf{7} \underset{\text{pH } \sim 9.1}{\overset{OH^-}{\rightleftharpoons}} \mathbf{8} \xrightarrow[\text{pH} > 11.2]{OH^-} \text{insoluble precipitates} \quad (3)$$

The presence of monodentate or bidentate TMDT complexes at low pH is not excluded by the ESR spectra.

[(TMDT)Cu(1-MeIm)](ClO$_4$)$_2$. Frozen solutions of this complex also display nearly axial ESR spectra at 77 K indicative of mixtures. The $g_\parallel$ and $A_\parallel$ values are collected in Table VI. Although **10** is a major component of the mixture around

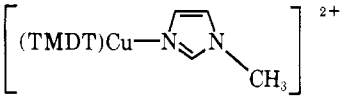

10

neutral pH, **9** forms at low pH and **8** is clearly present at pH ~11.2. Although the $A_\parallel$ values of **7** and **10** are both ~180 G, the $g_\parallel$ of **10** is 2.212 compared with 2.230 for **7**. The presence of a fourth nitrogen donor in the copper coordination plane also reduces the $g_\parallel$ value of the imidazolate bridged complex (vide infra). The ESR spectra are consistent with eq 4 and 5 for low

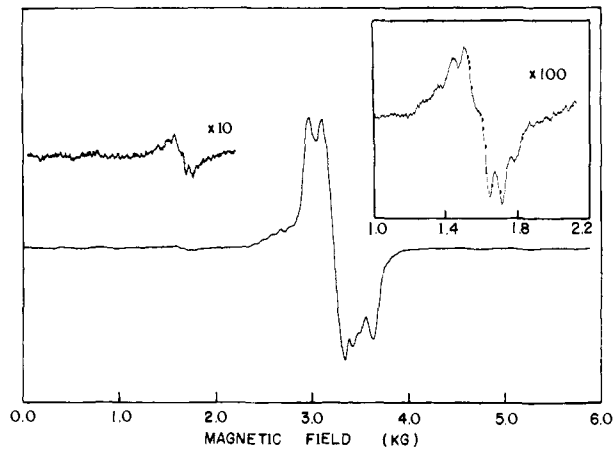

Figure 5. The ESR spectrum of a powdered sample of $[(TMDT)_2Cu_2(im)(ClO_4)_2](ClO_4)$ at 21.6 K. Instrumental settings were as reported for Figure 4 except that 5 mW of microwave power was used and the sweep rate was 2500 G/min. The inset shows the $\Delta M = 2$ transition at increased gain.

$$\mathbf{10} \underset{\text{pH } \sim 7.0}{\overset{H^+}{\rightleftharpoons}} \mathbf{7} + \text{1-MeImH}^+ \underset{\text{pH } \sim 2.6}{\overset{3H^+}{\rightleftharpoons}} \mathbf{9} + H_3(TMDT)^{3+} \quad (4)$$

$$\mathbf{10} \underset{\text{pH } \sim 10.5}{\overset{OH^-}{\rightleftharpoons}} \mathbf{8} + \text{1-MeIm} \xrightarrow[\text{pH} > 11.2]{OH^-} \text{insoluble precipitates} \quad (5)$$

and high pH solutions, respectively. It may be noted (Table VI) that the hydroxo complex **8** has become a major component in solutions of **7** at pH 9.1 whereas higher pH is required to form **8** from **10.** This result implies that 1-MeIm is a better ligand than water for $(TMDT)Cu^{2+}$.

$[(TMDT)_2Cu_2(im)(ClO_4)_2](ClO_4)$. The ESR spectrum of a powdered sample of this complex at 21.6 K is shown in Figure 5. Since the cation **6** contains two spin-coupled, axially symmetric copper(II) centers, both $\Delta M = 1$ and $\Delta M = 2$ transitions are expected.[32] For $\Delta M = 1$ transitions, calculations predict two groups of peaks spaced on either side of $g \sim 2$, with the overall width of the resonance determined by r, the distance between the copper(II) centers.[33] As r increases, the spectra narrow. The large r value of 5.935 Å in **6** produces a fairly narrow $\Delta M = 1$ resonance on an X-band spectrometer (Figure 5). The weak lines at ~2550 G result from a small amount of mononuclear cupric ion. A spectrum at 9 K confirmed this assignment since, at low temperatures, the imidazolate bridged complex is in the singlet ground state and does not exhibit ESR lines. Because of the presence of mononuclear copper(II) and the lack of a complete theory[32] for analyzing the spectra of bridged copper(II) dimers having $|J| > 15\ cm^{-1}$, no attempt was made to simulate the 21.6 K spectrum and obtain spectral parameters. The pronounced feature ~3570 G is characteristic of the imidazolate bridged dicopper(II) moiety, however, and this result is useful in interpreting the solution ESR spectra of **6,** as will be demonstrated.

The spin states for the $\Delta M = 2$ transitions are degenerate in the absence of a magnetic field and the ESR spectrum in the $\Delta M = 2$ region is, to first order, independent of the zero-field splitting. The $\Delta M = 2$ transitions occur at ~1500 G and have a low transition probability, being spin forbidden. In a system such as **6** with a fairly large exchange parameter $|J|$, the 16-line $[(2I_1 + 1)(2I_2 + 1)$, where $I_1 = I_2 = 3/2$ for the copper nucleus] hyperfine interaction will simplify to a seven-line $[2(I_1 + I_2) + 1]$ pattern with relative intensities in the ratio of 1:2:3:4:3:2:1 and a hyperfine spacing one-half that of the spectrum due to the individual copper(II) components.[32] As may be seen in Figure 5, the $\Delta M = 2$ resonance occurs at ~1530 G as a symmetric seven-line pattern with a hyperfine splitting of ~80 G.

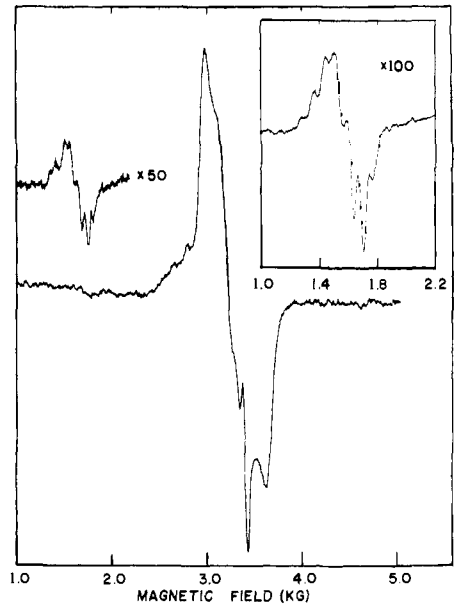

Figure 6. ESR spectrum of an ~10 mM frozen (77 K) 50% aqueous Me_2SO solution of $[(TMDT)_2Cu_2(im)(ClO_4)_2](ClO_4)$ at pH 8.5. Instrumental settings were as reported in the caption to Figure 4 except that a sweep rate of 2500 G/min was used. The inset displays the $\Delta M = 2$ region of the spectrum (×100) recorded at 50 K with 20 mW of microwave power, a 1-s time constant, and a sweep rate of 250 G/min.

The 77 K ESR spectrum of a frozen 50% aqueous Me_2SO solution of $[(TMDT)_2Cu_2(im)(ClO_4)_2](ClO_4)$, pH ~8.5, is given in Figure 6 with an expanded version of the $\Delta M = 2$ region taken at 50 K shown as an inset. Although a small amount of **6** has dissociated into mononuclear components **7** and **11,**

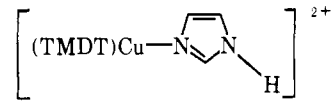

11

judging from the sharp line at 3365 G, the major constituent in solution is the bridged complex.[31] The pronounced feature at ~3570 G is identical with that observed in the powder spectrum (Figure 5). Moreover, seven copper hyperfine lines with an average spacing of 77 G appear on the $\Delta M = 2$ transition ~ 1520 G (Figure 6). The temperature dependence of this ESR spectrum is shown in Figure 7. At the lowest temperature, ~9 K, peaks of mononuclear complexes such as **7** and **11** with $g_\parallel \sim 2.218$ and $A_\parallel \sim 180$ G dominate the spectrum. The peaks due to the bridged complex **6** grow in as the temperature increases. This behavior is expected since at low temperatures the ground state of **6** is a singlet and will not contribute to the ESR spectrum. In principle, the exchange coupling parameter J can be determined from the temperature dependence of the ESR absorption intensity. This exercise was not attempted, however, since nonbridged species also exist in the frozen solution and, more importantly, the J value is accurately known from the susceptibility study.

Figure 8 shows the pH-dependent ESR spectra of frozen solutions of **6** at 77 K. Spectral parameters in the $g_\parallel$ region are included in Table VI. Decreasing the pH will sequentially break the imidazolate bridge,[8,10,11] release the imidazolium ion, and ultimately produce free cupric ion and $H_3(TMDT)^{3+}$:

$$\mathbf{6} \underset{\text{pH } \sim 8.0}{\overset{H^+}{\rightleftharpoons}} \mathbf{7} + \mathbf{11} \underset{\text{pH } \sim 7.0}{\overset{H^+}{\rightleftharpoons}} 2\,\mathbf{7} + imH_2^+ \underset{\text{pH } \sim 2.6}{\overset{6H^+}{\rightleftharpoons}} 2\,\mathbf{9} + 2H_3(TMDT)^{3+} \quad (6)$$

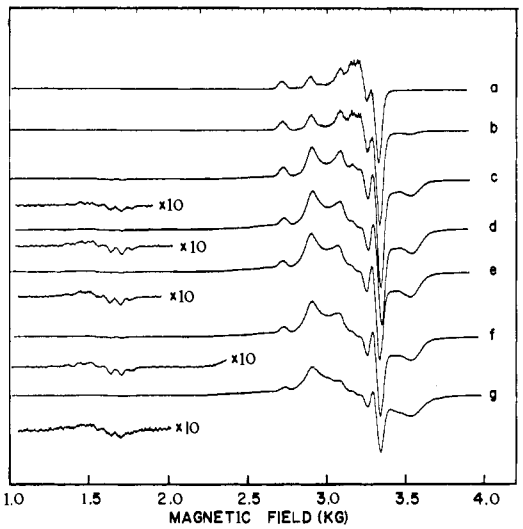

Figure 7. Temperature dependence of the ESR spectrum of ~10 mM $[(TMDT)_2Cu_2(im)(ClO_4)_2](ClO_4)$ in 50% Me_2SO/water, pH 9.1, at (a) 9.2 K, (b) 13.3 K, (c) 21.2 K, (d) 42.8 K, (e) 45.2 K, (f) 50.7 K, (g) 125.2 K. Instrumental conditions are the same as for Figure 4 except that 4 mW of microwave power was used.

As may be seen from Table VI and Figure 8, the intensities of the transitions due to the imidazolate bridged complex are diminished at low pH. Although the $A_\parallel$ value of 180 G cannot distinguish the mononuclear complexes in these frozen solutions, the $g_\parallel$ of 2.232 suggests that **11** dissociates readily to form **7** in the pH region (below 7.0) where the imidazolate bridge is broken. This resonance sharpens with decreasing pH as the **11** → **7** transition is completed. At very low pH, ~2.3, free copper(II) ion is easily identified by its small $A_\parallel \sim 119$ G and distinctive $g_\parallel$ and $g_\perp$ values of 2.412 and 2.099, respectively.

The ESR spectra of **6** in the high pH region (Figure 8) may be interpreted according to

$$\mathbf{6} \underset{\text{pH } \sim 10.5}{\overset{OH^-}{\rightleftharpoons}} \mathbf{8} + \mathbf{12} \underset{\text{pH } \sim 11.4}{\overset{H_2O}{\rightleftharpoons}} 2\,\mathbf{8} + \text{imH}$$

$$\xrightarrow[\text{pH} > 11.4]{OH^-} \text{insoluble precipitates} \qquad (7)$$

The binuclear bridged complex is a major component of the solution mainly in the narrow range $8.5 \lesssim \text{pH} \lesssim 9.5$. At higher pH values, the hydroxide ion will break the bridge to form species **8** and **12.** Loss of **6** with increasing pH is readily followed by observing the intensity diminution of the ~3570 G spectral feature and the concomitant appearance of the $g_\parallel$ resonances of **8** and **12.** Although these cannot be resolved, the

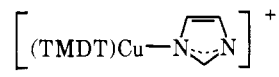

12

presence of **12** may be inferred by comparing the spectral details of **6** with those of **7** in the high pH range (Table VI and Figures 4 and 8). At higher pH, >11.4, a brown precipitate deposits.

Electronic Spectra. The optical absorption spectrum of $[(TMDT)_2Cu_2(im)(ClO_4)_2](ClO_4)$, dissolved to a concentration of 1.825 mM in water with a measured pH of 8.8 and diluted 1:1 with Me_2SO, has absorbance maxima at 278 and 624 nm with molar extinction coefficients of 1.02×10^4 and 390, respectively. The visible band of the ~10 mM concentration solutions used in the ESR spectral study shifts with pH, as listed in Table VI. Because of the occurrence of the equilibria shown in eq 6 and 7, the optical spectral band positions

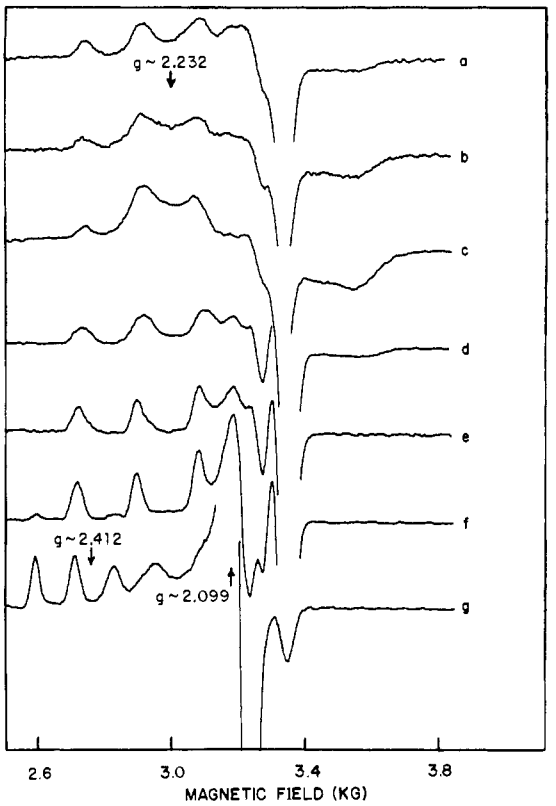

Figure 8. The ESR spectra of ~10 mM $[(TMDT)_2Cu_2(im)(ClO_4)_2](ClO_4)$ in frozen (77 K) 50% aqueous Me_2SO solutions at (a) pH 11.2, (b) pH 10.5, (c) pH 10.0, (d) pH 8.1, (e) pH 5.3, (f) pH 3.7, (g) pH 2.3. The instrumental conditions are described in the caption to Figure 4.

vary with concentration. The visible spectral band of **6** dissolved in pure water varies with pH in a manner analogous to that shown in Table VI for 50% aqueous Me_2SO solutions but with a 3-5-nm shift to longer wavelengths.

Discussion

Discrete imidazolate bridged dicopper(II) complexes are relatively easy to prepare using tridentate ligands such as TMDT, bpim (**3**), or pip (**5**)[10,11] to block oligomerization reactions. The imidazolate ion is generated in situ from imH by addition of 1 equiv of base. Chloride has been specifically avoided as a counterion because of its propensity to form bridged complexes. Antiferromagnetic spin exchange interactions[34] in di-μ-chloro-dicopper(II) ions would interfere with the use of magnetic criteria to identify μ-imidazolato-dicopper(II) centers.

For ligands such as bpim, the imidazolate ligand is constrained to lie in or nearly parallel to the copper coordination plane (**3, 4**). The imidazolate rings in the bridged complexes **5** and **6,** however, are nearly perpendicular to the copper coordination plane, and nonbonded steric interactions prohibit rotation about the Cu-N bonds. The magnetic properties of these two structurally different classes of imidazolate bridged dicopper(II) moieties have already been shown to differ substantially.[11] Free rotation about the Cu-N bonds to the bridging imidazolate ligand is also restricted by steric interactions in $[(TMDT)_2Cu_2(im)(ClO_4)_2](ClO_4)$.

The J value of -25.80 (16) cm^{-1} found from the susceptibility vs. temperature plot of solid **6** agrees nicely with the value of -26.74 (6) cm^{-1} reported previously for **5**.[11] This result does not help to clarify the extent to which π interactions contribute to the spin exchange mechanism, however, since the bridging ligand geometries of **5** and **6** are quite similar (see discussion in ref 11). Antiferromagnetic coupling constants of ~ -26 cm^{-1} appear to be characteristic of the $[Cu_2(im)]^{3+}$ moiety

in which the copper atoms are coordinated to four approximately planar donor atoms (including the nitrogen atom of the bridging imidazolate ligand) with one or two additional weak axial bonds. Ligands such as bpim (**3**), which produce a very different geometry for the $[Cu_2(im)]^{3+}$ center, lead to stronger antiferromagnetic coupling.[11] The g value of 2.085 ± 0.006 obtained from fitting the magnetic data to eq 1 is in reasonable agreement with the average g values of 2.074 and 2.107 estimated respectively from the powder (Figure 5) and frozen solution (Figure 6) ESR spectra of **6** in the $\Delta M = 1$ transition region.

The imidazolate bridged dicopper(II) center in $[(TMDT)_2Cu_2(im)(ClO_4)_2](ClO_4)$ has a distinctive ESR spectrum (Figures 5 and 6). Seven copper hyperfine lines are clearly resolved on the weak $\Delta M = 2$ transition. The $\Delta M = 1$ region of this spectrum has a characteristic feature at ~3570 G on an X-band spectrometer. As the temperature is lowered, the intensities of these ESR transitions diminish as more of the singlet ground state becomes populated (Figure 7). Mononuclear complexes such as **7** or **9** have axial or nearly axial ESR spectra (Figure 4) and are easily distinguished from **6**.

Optical spectroscopic and low-temperature ESR studies of 50% aqueous Me_2SO solutions show the imidazolate bridged complex to exist mainly over the narrow range $8.5 \lesssim pH \lesssim 9.5$ (Figures 6 and 8; Table VI). At low pH the imH_2^+ ion and mononuclear copper complexes form. Above pH 9.5 hydroxide ion splits the imidazolate bridge. The presence of mononuclear complexes is readily detected in the ESR spectra of frozen solutions (Figure 8) and by the shift to longer wavelengths of the copper d → d transition (Table VI). The latter occurs because imidazolate ion produces a stronger ligand field than water or hydroxide ion. At very low pH (~2.3) the TMDT ligand is released and the ESR spectrum is that of free cupric ion, **9** (Figure 8g).

These equilibria have been summarized in eq 6 and 7 and are supported by the pH-dependent studies of $[(TMDT)Cu(NO_3)](PF_6)$ and $[(TMDT)Cu(1\text{-MeIm})](ClO_4)_2$ using frozen solution ESR spectroscopy (cf. eq 2-5). The reactions shown in eq 6 and 7 will be dependent upon the total copper concentration. Thermodynamic constants might be accessible through potentiometric titrations even though a large number of copper(II) species are possible. Such studies of the methylmercury(II)-imidazole system have recently been published.[15] It is interesting that, like **6**, $[CH_3Hg]_2(im)^+$ is most stable at alkaline pH. Its greatest fractional concentration, referred either to all imidazole or to all methylmercury containing species in 10 mM solutions, occurs at pH ~9.2.

The magnetic and ESR spectral properties of **6** are remarkably similar to those of the derivative of BESOD in which zinc(II) has been replaced by copper(II) in both subunits of the protein.[16] The exchange coupling constant of -26 cm^{-1} in Cu_4BESOD agrees with the value of -25.80 (16) cm^{-1} in **6** and the ESR spectrum of the protein is nearly superimposable on that shown in Figure 6 (cf. Figure 3 of ref 16). These magnetic and ESR spectral properties can therefore be used (with appropriate caution) to identify imidazolate bridged dicopper(II) centers in proteins of unknown structure. Moreover, if the correlation[11] between the magnitude of the exchange coupling constant and the angles α_1 and α_2 made by the plane of the imidazolate ligand with the two copper coordination planes holds true, it follows that the angles for Cu_4-BESOD should be ~90°. It is noteworthy in this regard that the electron density maps of native Cu_2Zn_2BESOD show the imidazolate rings of the histidine bridge to have α ~0° with respect to the copper coordination plane.[3c] Thus either the 3-Å maps have insufficient resolution to reveal the correct orientation of the bridging imidazolate ring or the conformation of Cu_4BESOD differs from that of the native protein.

It is not an easy matter to assay complexes such as **6** for superoxide dismutase activity since even small amounts of cupric ion impurities will interfere.[35] As discussed above, samples that are completely free of mononuclear copper(II) are virtually impossible to prepare. In the enzyme assays, EDTA is used to complex free copper and inhibit its SOD activity.[35,36] Addition of EDTA to solutions of **6** rapidly destroys the complex. Studies of **6** and related complexes with superoxide ion are currently in progress.

An interesting finding in the present investigation of possible relevance to previous studies of BESOD is the fact that the imidazolate bridge can be broken by hydroxide ion at $pH \gtrsim 9.5$ as well as at low pH. The $E^{0\prime}$ value of BESOD is pH dependent in the range 5.5-8.7, suggesting that a proton is taken up as copper is reduced, viz., $ECu^{II} + e^- + H^+ \rightleftharpoons HECu^{I}$.[37] It is likely that the bridging imidazolate ligand is the proton receptor and that the pH independence of $E^{0\prime}$ below pH 5.5 is due to the fact that the histidine bridge is broken under these more acidic conditions.[5,38] Although no $E^{0\prime}$ data were reported for pH >9, the present results suggest that the redox potential should become independent of pH under basic conditions as hydroxide ion splits the imidazolate bridge.

The mononuclear complexes $[(TMDT)Cu(1\text{-MeIm})](ClO_4)_2$ and $[(TMDT)Cu(NO_3)](PF_6)$ were prepared to facilitate the identification of mononuclear species such as **7** and **11** generated through imidazolate bridge splitting reactions in aqueous solutions of **6**. Numerous monokiscopper(II) complexes of diethylenetriamine and its N-alkylated derivatives have been characterized.[27] All three TMDT complexes exhibit a strong, sharp absorption at ~3200 cm^{-1} in their solid state infrared spectra which is assigned to the N-H stretching frequency. Two N-H stretching bands (3244 and 3140 cm^{-1}) are present in the spectrum of $[(TMDT)Cu(1\text{-MeIm})](ClO_4)_2$. These may result from two different conformational isomers having the *N*-methyl substituent on the same or on opposite sides of the copper coordination plane as the N-H bond of the TMDT ligand; a perchlorate ion would probably coordinate on the same side as the *N*-methyl group (cf. discussion of the structure of **6**), further contributing to the shift in the N-H stretching frequency. The crystal structure determination of $[(TMDT)_2Cu_2(im)(ClO_4)_2](ClO_4)$ reveals both ionic and monodentate coordinated perchlorate, a feature that complicates the infrared spectrum in the Cl-O stretching frequency region (900-1200 cm^{-1}).[39] Infrared spectral similarities between this compound and $[(TMDT)Cu(1\text{-MeIm})](ClO_4)_2$ suggest that perchlorate ion also coordinates to copper in the 1-methylimidazole complex. Infrared absorptions at 1483, 1283, and 807 cm^{-1} in $[(TMDT)Cu(NO_3)](PF_6)$ are consistent with the presence of coordinated, probably bidentate, nitrate.[40]

Acknowledgments. This work was supported by Grant CHE76-18434 from the National Science Foundation and by NIH Research Grant GM-16449 from the National Institute of General Medical Sciences. We thank G. Kolks, P. Coughlin, and P. W. R. Corfield for helpful discussions and experimental advice, and D. N. Hendrickson, C. A. Reed, and S. S. Isied for preprints of their unpublished work.

Supplementary Material Available: Tables S1-S5 reporting the hydrogen atom positional parameters, refined thermal parameters, observed and calculated structure factor amplitudes, root-mean-square thermal amplitudes, and mean plane calculations for the $[(TMDT)_2Cu_2(im)(ClO_4)_2](ClO_4)$ crystal structure analysis; also, Figure S1 which contains a stereoview of the unit cell packing (16 pages). Ordering information is given on any current masthead page.

References and Notes

(1) Abbreviations: TMDT, 1,1,7,7-tetramethyldiethylenetriamine; imH, imidazole; im, imidazolate ion; 1-MeIm, 1-methylimidazole; BESOD, bovine erythrocyte superoxide dismutase; ESR, electron spin resonance; Me_2SO, dimethyl sulfoxide.

(2) (a) Columbia University; (b) IBM Yorktown Heights.
(3) (a) J. S. Richardson, K. A. Thomas, B. H. Rubin, and D. C. Richardson, *Proc. Natl. Acad. Sci. U.S.A.*, **72**, 1349 (1975); (b) K. M. Beem, D. C. Richardson, and K. V. Rajagopalan, *Biochemistry*, **16**, 1930 (1977); (c) D. C. Richardson, private communication. It should be noted that the existence of both Cu–N and Zn–N bonds to the imidazole ring of the histidine interposed between the metals is uncertain from the current, 3-Å X-ray results on BESOD.
(4) (a) W. H. Vanneste, *Biochemistry*, **5**, 838 (1966); (b) G. Palmer, G. T. Babcock, and L. E. Vickery, *Proc. Natl. Acad. Sci. U.S.A.*, **73**, 2206 (1976); (c) M. F. Tweedle, L. J. Wilson, L. Garcia-Iniquez, G. T. Babcock, and G. Palmer, Abstracts, 175th National Meeting of the American Chemical Society, Anaheim, Calif., March 13–17, 1978, No. INOR-59.
(5) (a) E. K. Hodgson and I. Fridovich, *Biochemistry*, 14, 5294 (1975), (b) S. J. Lippard, A. R. Burger, K. Ugurbil, J. S. Valentine, and M. W. Pantoliano, *Adv. Chem. Ser.*, **162**, 251 (1977); (c) M. E. McAdam, E. M. Fielden, F. Lavelle, L. Calabrese, D. Cocco, and G. Rotilio, *Biochem. J.*, **167**, 271 (1977).
(6) M. Inoue and M. Kubo, *Coord. Chem. Rev.*, **21**, 1 (1976).
(7) C. Creutz and H. Taube, *J. Am. Chem. Soc.*, **95**, 1086 (1973).
(8) R. J. Sundberg and R. B. Martin, *Chem. Rev.*, **74**, 471 (1974).
(9) (a) J. A. Jarvis and A. F. Wells, *Acta Crystallogr.*, **13**, 1027 (1960); (b) G. P. Brown and S. Aftergut, *J. Polym. Sci., Part A*, **2**, 1839 (1964); (c) J. E. Bauman, Jr., and J. C. Wang, *Inorg. Chem.*, **3**, 368 (1964), and references cited therein; (d) M. Inoue, M. Kishita, and M. Kubo, *ibid.*, **4**, 626 (1965); *Bull. Chem. Soc. Jpn.*, **39**, 1352 (1966); (e) W. J. Eilbeck, F. Holmes, and A. E. Underhill, *J. Chem. Soc. A*, 757 (1967); (f) C. I. Brändén and C. Sandmark, unpublished results quoted in H. C. Freeman, *Adv. Protein Chem.*, **22**, 257 (1967); (g) F. Seel and V. Sperber, *Angew. Chem., Int. Ed. Engl.*, **7**, 70 (1968); (h) C. Sigwart, P. Kroneck, and P. Hemmerich, *Helv. Chim. Acta*, **53**, 177 (1970); (i) K.-H. Thiele and M. Bendull, *Z. Anorg. Allg. Chem.*, **379**, 199 (1970); (j) E. Baraniak, H. C. Freeman, J. M. James, and C. E. Nockolds, *J. Chem. Soc. A*, 2558 (1970); (k) M. E. Bridson and W. R. Walker, *Aust. J. Chem.*, **23**, 1973 (1970); (l) S. Sjöberg, *Acta Chem. Scand.*, **25**, 2149 (1971); (m) G. Ivarsson, B. K. S. Lundberg, and N. Ingri, *ibid.*, **26**, 3005 (1972); (n) B. K. S. Lundberg, *ibid.*, **26**, 3902 (1972); (o) F. Seel, P. Wende, A. Trautwein, H. E. Marcolin, and Y. Maeda, *Z. Anorg. Allg. Chem.*, in press (results quoted in H. E. Marcolin, A. Trautwein, Y. Maeda, F. Seel, and P. Wende, *Theor. Chim. Acta*, **41**, 223 (1976)); (p) M. Inoue and M. Kubo, *J. Coord. Chem.*, **6**, 157 (1977).
(10) G. Kolks, C. R. Frihart, H. N. Rabinowitz, and S. J. Lippard, *J. Am. Chem. Soc.*, **98**, 5720 (1976).
(11) G. Kolks and S. J. Lippard, *J. Am. Chem. Soc.*, **99**, 5804 (1977).
(12) M. S. Haddad and D. N. Hendrickson, *Inorg. Chem.*, **17**, 2622, (1978).
(13) (a) J. T. Landrum, C. A. Reed, K. Hatano, and W. R. Scheidt, *J. Am. Chem. Soc.*, **100**, 3232 (1978); (b) M. Nappa, J. S. Valentine, and P. A. Snyder, *ibid.*, **99**, 5799 (1977).
(14) (a) C. A. Evans, D. L. Rabenstein, G. Geier, and I. W. Erni, *J. Am. Chem. Soc.*, **99**, 8106 (1977); (b) D. L. Rabenstein, *Acc. Chem. Res.*, **11**, 100 (1978).
(15) S. S. Isied and C. G. Kuehn, submitted for publication.
(16) J. A. Fee and R. G. Briggs, *Biochim. Biophys. Acta*, **400**, 439 (1975).
(17) S. Krasney and H. R. Lilienthal, IBM Thomas J. Watson Research Center Report RC 5504, 1975.
(18) B. N. Figgis and J. Lewis in "Modern Coordination Chemistry", J. Lewis and R. G. Wilkins, Ed., Interscience, New York, N.Y., 1960, p 400 ff.
(19) "International Tables for X-ray Crystallography", Vol. I, 2nd ed., Kynoch Press, Birmingham, England, 1965, pp 79 and 93.
(20) "International Tables for X-ray Crystallography", Vol. IV, Kynoch Press, Birmingham, England, 1974, pp 72–79, 149.
(21) R. F. Stewart, E. R. Davidson, and W. T. Simpson, *J. Chem. Phys.*, **42**, 3175 (1965).
(22) $R_1 = \Sigma||F_o| - |F_c||/\Sigma|F_o|$ and $R_2 = [\Sigma w(|F_o| - |F_c|)^2/\Sigma w|F_o|^2]^{1/2}$, where $w = 4F_o^2/\sigma^2(F_o^2)$. In the least-squares refinement, the function $\Sigma w(|F_o| - |F_c|)^2$ was minimized.
(23) D. W. J. Cruickshank in "Computing Methods of Crystallography", J. S. Rollett, Ed., Pergamon Press, Elmsford, N.Y., 1965, pp 112–115.
(24) Supplementary material.
(25) Several apparently crystalline imidazolate bridged dicopper(II) complexes examined in our laboratory have either shown complex diffraction patterns indicative of twinning or have proved to be badly disordered (cf. ref 11, footnote 8). Even the present crystals were only marginally satisfactory.
(26) (a) H. C. Freeman and J. T. Szymanski, *Acta Crystallogr.*, **22**, 406 (1967); (b) D. L. McFadden, A. T. McPhail, C. D. Garner, and F. E. Mabbs, *J. Chem. Soc., Dalton Trans.*, 263 (1975).
(27) (a) F. S. Stephens, *J. Chem. Soc. A*, 2493 (1969); (b) G. Davey and F. S. Stephens, *ibid.*, 103 (1971); (c) J. W. Allison and R. J. Angelici, *Inorg. Chem.*, **10**, 2233 (1971); (d) M. J. Bew, B. J. Hathaway, and R. J. Fereday, *J. Chem. Soc., Dalton Trans.*, 1229 (1972); (e) B. G. Segal and S. J. Lippard, *Inorg. Chem.*, **13**, 822 (1974); (f) T. R. Felthouse and D. N. Hendrickson, *ibid.*, **17**, 444 (1978); and references cited therein.
(28) See, for example, C. C. Ou, V. M. Miskowski, R. A. Lalancette, J. A. Potenza, and H. J. Schugar, *Inorg. Chem.*, **15**, 3157 (1976).
(29) A. P. Ginsberg, *Inorg. Chim. Acta Rev.*, **5**, 45 (1971).
(30) B. Bleany and K. D. Bowers, *Proc. R. Soc. London, Ser. A*, **214**, 451 (1952).
(31) Both water and Me_2SO are likely to be coordinated in fifth and possibly sixth coordination positions for **7–9** and analogous species discussed later. Although water is shown as the ligand in **7**, Me_2SO may be coordinated instead. It is not possible from the ESR spectra to distinguish these two potential ligands.
(32) T. D. Smith and J. R. Pilbrow, *Coord. Chem. Rev.*, **13**, 173 (1974), and references cited therein.
(33) J. F. Boas, R. H. Dunhill, J. R. Pilbrow, R. C. Srivastava, and T. D. Smith, *J. Chem. Soc. A*, 94 (1969). Although these calculations apply, strictly speaking, only to spin-coupled systems having $|J| \lesssim 15\ cm^{-1}$, the gross features will probably be retained for the present case where $J = -25.8\ cm^{-1}$.
(34) D. J. Hodgson, *Prog. Inorg. Chem.*, **19**, 173 (1975).
(35) J. A. Fee, R. Natter, and G. S. T. Baker, *Biochim. Biophys. Acta*, **295**, 96 (1973).
(36) (a) J. M. McCord and I. Fridovich, *J. Biol. Chem.*, **244**, 6049 (1969); (b) D. Klug, J. Rabani, and I. Fridovich, *ibid.*, **247**, 4839 (1972).
(37) J. A. Fee and P. E. DiCorleto, *Biochemistry*, **12**, 4893 (1973).
(38) J. A. Fee in "Superoxide and Superoxide Dismutases", A. Michelson, J. M. McCord, and I. Fridovich, Ed., Academic Press, New York, N.Y., 1977, pp 173–192.
(39) K. Nakamoto, "Infrared Spectra of Inorganic and Coordination Compounds", 2nd ed., Wiley-Interscience, New York, N.Y., 1970, p 176.
(40) (a) N. F. Curtis and Y. M. Curtis, *Inorg. Chem.*, **4**, 804 (1965); (b) ref 39, p 172.

Preparation and Chemistry of Some Phosphoranes Containing Phosphorus–Sulfur Bonds

Byron C. Burros, Norman J. De'Ath, Donald B. Denney,* Dorothy Z. Denney, and Irving J. Kipnis

Contribution from the Department of Chemistry, Rutgers, The State University of New Jersey, New Brunswick, New Jersey 08903. *Received April 24, 1978*

Abstract: The dithiete, **2**, has been allowed to react with a variety of trivalent phosphorus compounds. In some cases phosphoranes are formed which contain a five-membered ring with two sulfurs bonded to phosphorus. In others unstable phosphoranes may have been formed which then decomposed to a variety of products. Variable temperature NMR studies of the phosphoranes have been conducted. In most cases it was not possible to determine whether the materials are rapidly interconverting trigonal bipyramids or whether they are static or rapidly interconverting square or rectangular pyramids.

Thus far, very few pentacoordinate phosphorus compounds, phosphoranes,[1] have been prepared in which one or more sulfur atoms are bonded to phosphorus. Peake and Schmutzler[2] prepared a number of alkyl and arylthio substituted fluorophosphoranes and studied their variable temperature ^{19}F NMR spectra. They found at low temperatures that the alkylthio and arylthio groups prefer an equatorial position in the trigonal bipyramidal structure (TP) and that there is inhibition to rotation about the P–S bond.

More recently, Trippett and co-workers[3] prepared a series

0002-7863/78/1500-7300$01.00/0